

## First and Second Sound Modes of a Bose-Einstein Condensate in a Harmonic Trap

V. B. Shenoy and Tin-Lun Ho

*Department of Physics, The Ohio State University, Columbus, Ohio 43210*

(Received 19 November 1997)

We have calculated the first and second sound modes of a dilute interacting Bose gas in a spherical trap for temperatures ( $0.6 < T/T_c < 1.2$ ) and for systems with  $10^4$  to  $10^8$  particles. The second sound modes (which exist only below  $T_c$ ) generally have a stronger temperature dependence than the first sound modes. The puzzling temperature variations of the sound modes near  $T_c$  recently observed at JILA in systems with  $10^3$  particles match surprisingly well with those of the first and second sound modes of much larger systems. [S0031-9007(98)05981-X]

PACS numbers: 03.75.Fi, 05.30.Jp

Since the discovery of Bose-Einstein condensation in atomic gases of alkali atoms [1], there has been great interest in the broken gauge symmetry (i.e., the “phase”) of the condensate. In the case of  $^4\text{He}$ , its “phase” dynamics leads to the existence of second sound, which is essentially the out of phase pressure and temperature oscillations. In a series of sound experiments, Jin *et al.* at JILA [2] have observed a number of “puzzling” behaviors in the temperature dependence and the dissipation of the sound modes above  $0.5T_c$ . There are no explanations for these behaviors so far. Jin *et al.* have speculated that the observed “ $m = 0$ ” mode could be the “second sound.” If this were true, it would be consistent with (though not a proof of) the broken gauge symmetry of the system. However, in the absence of a detailed calculation consistent with experiments, the identification of the second sound mode would be difficult.

To help identify the nature of the sound modes, we have solved the linearized two-fluid hydrodynamic equations of an interacting dilute Bose gas in a spherical harmonic trap. We have in mind systems that are sufficiently large so that the hydrodynamic approach is accurate [3]. It should be noticed that the recent experiments at JILA [2] were performed on small systems with a few thousand atoms. While the hydrodynamic modes of a large system may be different from the sound modes of a small one, the study of the former is important in its own right. After all, the number of atoms in the Bose condensate has increased from  $10^3$  to  $10^6$  within six months after the initial discovery [1]. It would not be surprising if Bose condensates with  $10^9$  atoms were produced in the near future. On the other hand, the hydrodynamic modes of large systems *are* relevant for the sound modes of small ones, as the former must evolve smoothly into the latter as the number of atoms is decreased continuously. This suggests the possibility of identifying the nature of sound modes of a small system by studying their hydrodynamic counterparts in a large one. Indeed, comparing our results (for systems with  $10^4$  to  $10^8$  atoms) with the JILA observations [2], we find that

the temperature variations of the observed sound modes show up in the analogous modes of the larger systems in a spherical trap. In particular, the “mysterious” behaviors of the JILA ( $m = 0$ ) and ( $m = 2$ ) modes [2] in the range  $0.5 < T/T_{co} < 0.8$  match closely with the behaviors of the second sound modes of the larger systems in the same temperature range, while the frequency and temperature dependence of the observed ( $m = 0$ ) mode above  $T_c$  are identical to those of the first sound mode in the same temperature range. (The temperatures  $T_{co}$  and  $T_c$  are the transition temperature for the ideal Bose and the dilute interacting Bose gas, respectively [4]).

Our choice of spherical symmetry is to keep the calculations manageable. Moreover, as a first step, we shall ignore dissipation. While it is entirely feasible within our scheme to include dissipative effect, we feel that it is important (as in bulk  $^4\text{He}$ ) to first understand dissipationless hydrodynamics, so that one can clearly identify the dissipative effects later in a complete solution.

*Linearized hydrodynamics.*—We begin with the two-fluid hydrodynamic equations of Bosons with mass  $M$  in an external potential  $\phi(\mathbf{r})$  [5],  $M\dot{\mathbf{n}} = -\nabla \cdot \mathbf{g}$ ,  $\dot{g}_i = -n\nabla_i\phi - \nabla_j \Pi_{ij}$ ,  $\dot{s} = -\nabla \cdot (s\mathbf{v}_n)$ , and  $\dot{\mathbf{v}}_s = -\frac{1}{M}\nabla(\mu + \phi + M\mathbf{v}_n \cdot \mathbf{v}_s)$ , where  $n$ ,  $\mathbf{g}$ ,  $\Pi_{ij}$ ,  $s$ ,  $\mu$  are the number density, the momentum density, the stress tensor, the entropy density, and the chemical potential, respectively. Here,  $\mathbf{v}_n$  and  $\mathbf{v}_s \equiv (\hbar/M)\nabla\theta$  are the normal fluid and superfluid velocities, respectively, where  $\theta$  is the phase of condensate. For a spherical harmonic trap with frequency  $\omega_T$ ,  $\phi(r) = \frac{1}{2}M\omega_T^2 r^2$ . In the presence of a condensate,  $n$ ,  $\mathbf{g}$ , and  $\Pi_{ij}$  are of the form  $n = n_s + n_n$ ,  $\mathbf{g} = M(n_n\mathbf{v}_n$  and  $\Pi_{ij} = P\delta_{ij} + M(n_n v_{ni} v_{nj} + n_s v_{si} v_{sj})$ , where  $n_s$  and  $n_n$  are the superfluid and normal fluid number densities, and  $P$  is the pressure. Denoting the equilibrium quantities by the subscript “ $o$ ”, we have  $\mathbf{v}_{no} = \mathbf{v}_{so} = 0$ ,  $\nabla P_o + n_o \nabla \phi = 0$ , and  $\nabla(\mu_o + \phi) = 0$ . Using the Gibbs-Duhem relation  $d\mu = -\sigma dT + dP/n$ , where  $\sigma \equiv s/n$  is the entropy per particle, these equilibrium

conditions imply  $\nabla T_o = 0$ , and hence

$$\begin{aligned} \nabla n_o &= \left( \frac{\partial n}{\partial P} \right)_{T_o} \nabla P_o = -n_o \left( \frac{\partial n}{\partial P} \right)_{T_o} \nabla \phi, \\ \nabla \sigma_o &= \left( \frac{\partial \sigma_o}{\partial P} \right)_{T_o} \nabla P_o = -\frac{1}{n_o} \left( \frac{\partial n}{\partial T} \right)_{P_o} \nabla \phi, \end{aligned} \quad (1)$$

where we have made use of the Maxwell relation  $(\partial \sigma / \partial P)_T = n^{-2} (\partial n / \partial T)_P$ .

Denoting the deviation of any quantity  $x$  from its equilibrium value  $x_o$  as  $\delta x \equiv x - x_o$ , the hydrodynamic equations can be linearized about the equilibrium solution and written as I:  $\delta \dot{n} = -\nabla \cdot (n_o \mathbf{v}_s + n_{no} \mathbf{w})$ , II:  $n_o \dot{\mathbf{v}}_s + n_{no} \dot{\mathbf{w}} = -(\delta n \nabla \phi + \nabla \delta P) / M$ , III:  $\dot{\mathbf{v}}_s = \frac{1}{M} \nabla (\sigma_o \delta T - \frac{\delta P}{n_o})$ , IV:  $\delta \dot{s} = -\nabla \cdot (s_o \mathbf{v}_n)$ , where  $\mathbf{w} = \mathbf{v}_n - \mathbf{v}_s$ . Using Eq. (1), I and II imply that

$$M \delta \ddot{n} = \nabla \cdot \left[ n_o \nabla \left( \frac{\delta P}{n_o} \right) - \delta T n_o \nabla \sigma_o \right] \equiv A. \quad (2)$$

Again using Eq. (1), II and III, we have  $\dot{\mathbf{w}} = -\frac{n_o \sigma_o}{M n_{no}} \nabla \delta T$ . By noting that  $\dot{s} = \sigma_o \dot{n} + n_o \dot{\sigma}$ , it is easy to show from IV that  $\dot{\sigma} = -\dot{\mathbf{v}}_n \cdot \nabla \sigma_o - \frac{\sigma_o}{n_o} \nabla \cdot (n_{so} \dot{\mathbf{w}})$ , and hence

$$\begin{aligned} M \ddot{\sigma} &= -(\nabla \sigma_o)^2 \delta T + \frac{1}{n_o} \nabla \cdot \left( \frac{n_o n_{so} \sigma_o^2}{n_{no}} \nabla \delta T \right) \\ &+ \nabla \sigma_o \cdot \nabla \left( \frac{\delta P}{n_o} \right) \equiv B. \end{aligned} \quad (3)$$

Expressing all quantities in terms of  $\delta T$  and  $\delta P$ , Eqs. (2) and (3) form a closed set:  $(\frac{\partial n}{\partial P})_T \delta \ddot{P} + (\frac{\partial n}{\partial T})_P \delta \ddot{T} = A/M$ ,  $(\frac{\partial \sigma}{\partial P})_T \delta \ddot{P} + (\frac{\partial \sigma}{\partial T})_P \delta \ddot{T} = B/M$ . To solve them, we have calculated the thermodynamic quantities in these equations using local density approximation (LDA) [6] for the tem-

perature range  $a \lambda^2 n_o \ll 1$ , where  $\lambda \equiv \sqrt{2\pi \hbar^2 / M k_B T}$  is the thermal wavelength. As shown by Lee and Yang [7], all thermodynamic quantities within this range can be calculated analytically. With the coefficients of Eqs. (2) and (3) calculated in this manner, we then solve these equations numerically by discretizing them on a grid which is made finer as  $r \rightarrow r^*$ , where  $r^*$  is the interface between the condensate and the normal cloud. Bearing in mind that LDA collapses the interface into a single surface at  $r^*$ , we model the interface and the behavior of  $\delta P$  and  $\delta T$  as follows: The interface is modeled by three points  $r^* \pm \Delta$  and  $r^*$ , where  $\Delta$  is the grid spacing. Both  $\delta P$  and  $\delta T$  as well as their derivatives are continuous at  $r^*$ , while the values of  $\delta P$  and  $\delta T$  at  $r^* + \Delta$  and  $r^* - \Delta$  are determined by their solutions inside and outside  $r^*$ .

*Main results.*—Because of spherical symmetry,  $\delta P$  and  $\delta T$  can be decomposed as  $[\delta P(\mathbf{r}), \delta T(\mathbf{r})] = \sum_{\ell, n, m} [\delta P_{\ell n}(r), \delta T_{\ell n}(r)] Y_{\ell m}(\hat{\mathbf{r}})$ , where  $\ell$  is the angular momentum and  $n$  is the radial quantum number. Each  $(\ell, n)$  mode is  $2\ell + 1$  fold degenerate. We have performed calculations for  $^{87}\text{Rb}$  ( $a = 58.2 \text{ \AA}$ ) for  $N = 10^4$  to  $10^8$  atoms and have found identical general features. For all cases studied, *the frequencies of all first and second sound are above the trap frequency  $\omega_T$*  [3], which is to be expected if the system is viewed as a mechanical system with internal degrees of freedom in a spherical harmonic potential. For concreteness, we present the results for  $N = 10^6$  particles in a trap, with  $\omega_T / 2\pi = 200 \text{ Hz}$ , over the range  $0.6 < T/T_c < 1.2$ :

*A. First sound.*—These modes exist both above and below  $T_c$ . They are *in phase* pressure and temperature oscillations that extend over the entire cloud, and  $\delta P$  has

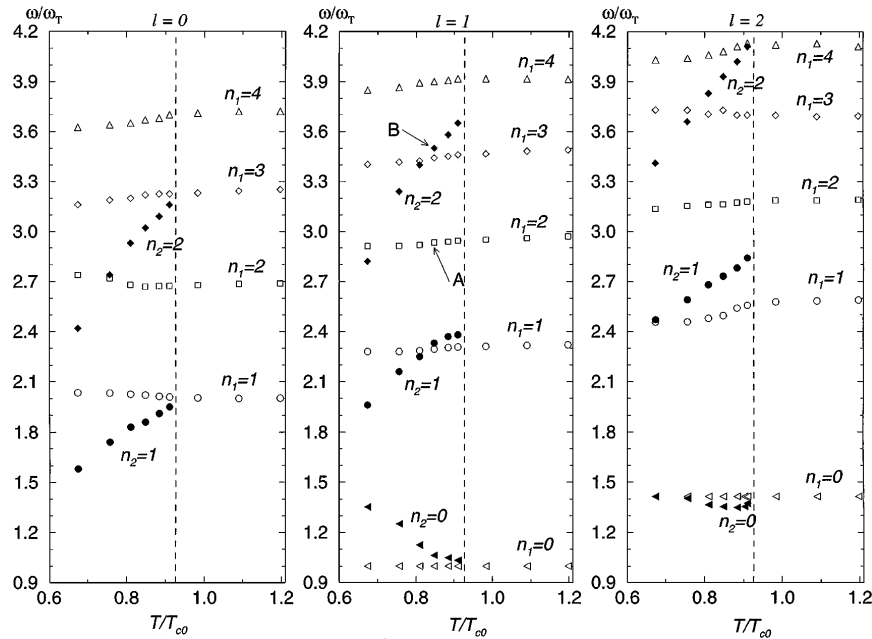


FIG. 1. The frequencies  $\omega_{\ell, n_1}^{(1)}$  and  $\omega_{\ell, n_2}^{(2)}$  are represented as open and filled symbols, respectively.  $T_{c0}$  is the transition temperature of the ideal Bose gas in the trap. The dotted line at  $0.917 T_{c0}$  indicates the critical temperature  $T_c$  of the interacting model. For the  $\ell \neq 0$  modes,  $r = 0$  is not counted as a node. As far as we can tell,  $\omega_{\ell=0, n_2=0} = 0$ .

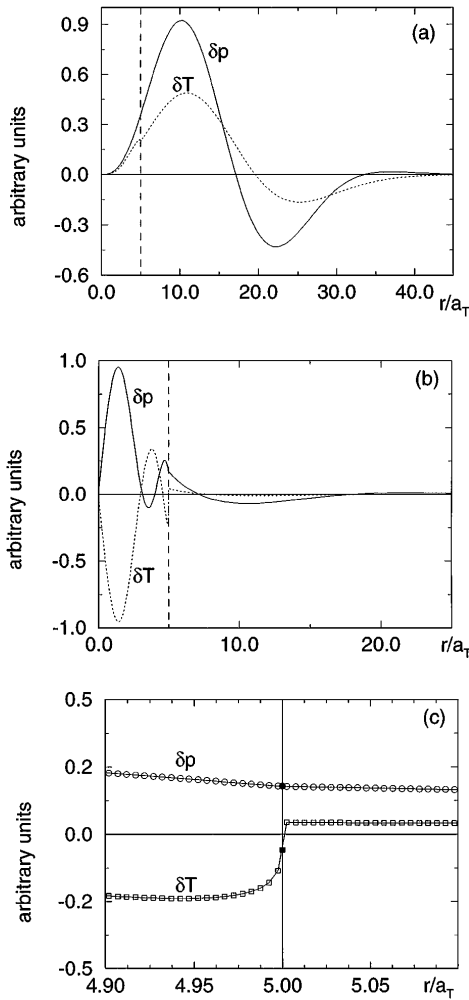


FIG. 2. (a) The eigenfunctions of  $\omega_{\ell=1, n_1=2}^{(1)}$  (marked as A in Fig. 1): To magnify the features of the first sound, we have multiplied  $\delta P$  and  $\delta T$  by  $r^2$  in (a). (b) The eigenfunctions of  $\omega_{\ell=1, n_2=2}^{(2)}$  (marked as B in Fig. 1): These functions are not multiplied by  $r^2$  as those in (a) because their features are sufficiently clear. (c) The detailed structure in (b) near  $r^*$ : The filled point indicates the location of  $r^*$ , and  $\Delta$  is  $0.005a_T$ . The sharp change of slope at  $r^* \pm \Delta$  is expected as out boundary condition is meant to simulate the collapsing process of LDA at  $r^*$ .

one more node than  $\delta T$ . The frequencies of these modes (denoted as  $\omega_{\ell n_1}^{(1)}$ ) are shown in Fig. 1 for  $\ell = 0, 1, 2$  and  $n_1 = 0$  to 4 where  $n_1$  counts the number of nodes of  $\delta P$  in the radial direction. While  $\{\omega_{\ell n_1}^{(1)}\}$  change with temperature, their variations are small compared to  $\omega_T$ . The eigenfunctions of the  $(\ell = 1, n_1 = 2)$  mode at  $T = 0.84T_{co}$  are shown in Fig. 2(a). They extend over the entire cloud—a feature common to all first sound modes above and below  $T_c$ .

The  $n_1 = 0$  modes are special. They are isothermal modes of the form  $\delta P(r, \hat{\mathbf{r}}) = n_o(r)r^\ell Y_{\ell m}(\hat{\mathbf{r}})$ ,  $\delta T = 0$ , with  $\omega_{\ell, 0}^{(1)} = \omega_T \sqrt{\ell}$ . They are also “universal” in the sense that they are *independent of interaction and statistics*. These results emerge from our numerical solutions

but can also be obtained analytically from Eqs. (2) and (3). With  $\delta T = 0$ , using the equilibrium relations given by Eqs. (1)–(3) can be shown to yield  $\nabla^2(\delta P/n_o) = 0$ , and  $\partial_t^2(\delta P/n_o) = -\nabla \phi \cdot \nabla(\delta P/n_o)$ , which has the solution given above. From the hydrodynamic equations I to IV, it is also straightforward to show that for these isothermal modes,  $\mathbf{v}_n = \mathbf{v}_s$  below  $T_c$ , and  $\nabla \cdot \mathbf{v}_n = 0$  both above and below  $T_c$ .

The  $(\ell = 0, n_1 = 1)$  mode is also special. Above  $T_c$ , it is a uniform temperature oscillation,  $\nabla \delta T = 0$ , but with  $\delta T \neq 0$ . This mode is “nonuniversal” because it depends on interaction. The interaction effect, however, is sufficiently weak so that  $\omega_{0,1}^{(1)}$  is very close to  $2\omega_T$  above  $T_c$ . It is also straightforward to show that  $\nabla \cdot \mathbf{v}_n$  is constant but nonzero for this mode. These results can be established analytically using LDA and also emerge as part of our numerical solutions. Below  $T_c$ ,  $\delta T$  is no longer uniform, and  $\nabla \cdot \mathbf{v}_n$  is not a constant [8]. All the other sound modes  $(\ell, n_1 \neq 0)$  are nonisothermal.

**B. Second sound.**—These modes exist only below  $T_c$ . The frequencies of these modes for  $(\ell = 0, 1, 2)$  and  $(n_2 = 0, 1, 2)$  are shown in Fig. 1. It should be stressed that the second sound frequencies do not merge into the first sound frequencies as  $T \rightarrow T_c$ . To illustrate this clearly, we plot  $\omega_{\ell, n_2=1}^{(2)}$  near  $T_c$  (for  $\ell = 0$  to 2) as a function of particle number  $N$  in Fig. 3. While  $\omega_{\ell, n_2=1}^{(2)}$  changes with  $N$ , the first sound frequencies (not shown in Fig. 3) typically vary by about 2% of  $\omega_T$  in the same range of  $N$ . The eigenfunctions of the  $(\ell = 1, n_2 = 2)$  mode are shown in Fig. 2(b). An enlarged structure of the interface of this mode at  $r^*$  is shown in Fig. 2(c). The second sound modes have the following common features: (1)  $\delta P$  and  $\delta T$  are “out of phase” inside the condensate and become “in phase” as they leak out into the normal region. The leakage reduces to zero as  $T \rightarrow T_c$ . The quantum number  $n_2$  counts the number of nodes of  $\delta P$  or  $\delta T$  inside the condensate. (2) The wavelengths of the oscillations shrink as  $r \rightarrow r^*$ . This can be understood simply from LDA by recalling that the second sound velocity  $c_2$  of a homogenous dilute Bose gas is proportional to  $\sqrt{n_{so}}$ . The wavelength  $2\pi k^{-1}$  is then  $2\pi c_2/\omega \propto \sqrt{n_{so}}$ . Since  $\omega \sim \omega_T$  in our case,

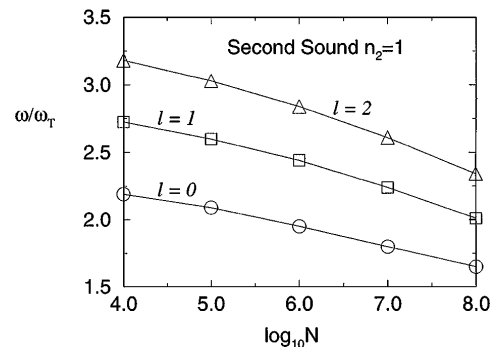


FIG. 3. The  $N$  dependence of  $\omega_{\ell, n_2=1}^{(2)}$  modes  $(\ell, n_2 = 1)$  near  $T_c$ . The temperature is chosen so that  $r^* = a_T$ .

and  $n_{so}(r)$  vanishes as  $r \rightarrow r^*$ , the local wavelength shrinks as  $r \rightarrow r^*$ . (3) The  $n_2 = 0$  modes are different from all other  $n_2 \neq 0$  modes. First, except very close to  $T_c$ , all  $\omega_{\ell, n_2 \neq 0}^{(2)}$  increase as  $T$  decreases, whereas all  $\omega_{\ell, n_2 \neq 0}^{(2)}$  have opposite behavior (see Fig. 1). Second, while  $\delta T$  and  $\delta P$  are out of phase for all second sound modes (i.e.,  $n_2 = 0$  and  $n_2 \neq 0$ ), the sign of  $\mathbf{v}_s \cdot \mathbf{v}_n$  for a particular mode depends on position. In particular,  $\mathbf{v}_s \cdot \mathbf{v}_n$  of the  $n_2 = 0$  modes is actually positive (i.e., in phase) almost everywhere inside the condensate instead of negative [3], whereas it can be positive or negative for the  $n_2 \neq 0$  modes. (The radial components of  $\mathbf{v}_s$  and  $\mathbf{v}_n$  for the  $n_2 \neq 0$  modes are out of phase in most regions in the condensate; so are their tangential components. However, the in-phase and out-of-phase regions of these two components do not coincide.) This shows that unlike the second sound modes in homogenous systems, which are characterized by either out of phase ( $\delta P, \delta T$ ), or out of phase ( $\mathbf{v}_s, \mathbf{v}_n$ ) oscillations, *the correct characterization of the second sound modes in the trap is the out of phase  $\delta P$  and  $\delta T$  oscillations, not the out of phase  $\mathbf{v}_s$  and  $\mathbf{v}_n$  oscillations* [3]. (4) Near the center of the cloud, the ratio  $\xi \equiv |n_n v_n / n_s v_s|$  is about 0.2 to 0.3 for the mode studied. This is very different from  $^4\text{He}$ , where the normal current is essentially canceled by the supercurrent, i.e.,  $\xi \equiv |n_n v_n / n_s v_s| \sim 1$  [3]. That  $\xi$  is between 0.2 and 0.3 can be understood in terms of LDA. From the work of Lee and Yang [9], one finds that  $\xi = \frac{12}{5}(a/\lambda)[g_{3/2}^2(1)/g_{5/2}(1)]$  for the homogeneous dilute Bose gas, which is around 0.3 for the temperature range studied [3]. (5) In terms of dimensionless quantities  $[\delta \tilde{P}, \delta \tilde{T}] \equiv (\delta P/[n_o(\mathbf{r})k_B T_o], \delta T/T_o)$ , we find that near  $T_c$ ,  $\delta \tilde{T}/\delta \tilde{P} \gg 1$  for all second sound modes, whereas  $\delta \tilde{P} \sim \delta \tilde{T}$  for the first sound modes.

*Comparison with the JILA data.*—Examining the JILA data [2] on the sound modes of  $^{87}\text{Rb}$  with  $\sim 2 \times 10^3$  atoms, we find surprising consistency with the behaviors of the larger systems that we studied: (a) A ( $m = 0$ ) mode with frequency  $\approx 2\omega_T$  was observed for all  $T$  above  $T_c$  [2]. The analog of this mode in a spherical trap is the ( $\ell = 0, n_1 = 1$ ) first sound mode, which also has frequency  $\approx 2\omega_T$  for all  $T$  above  $T_c$ . (b) Below  $T_c$ , the frequency of the ( $m = 0$ ) mode falls from about  $2\omega_T$  to  $1.85\omega_T$  as  $T$  decreases from  $0.9T_{co}$  to  $0.5T_{co}$  [2]. The first and second sound analogs of this mode below  $T_c$  are the ( $\ell = 0, n_1 = 1$ ) and the ( $\ell = 0, n_2 = 1$ ) modes, respectively. The observed behavior matches well with the ( $\ell = 0, n_2 = 1$ ) second sound mode, which drops from about  $1.9\omega_T$  to  $1.5\omega_T$  as  $T$  decreases from  $0.8T_{co}$  to  $0.6T_{co}$  as seen from Fig. 1. (c) An ( $m = 2$ ) mode was also observed below  $T_c$  [2]. Its frequency decreases from  $1.45\omega_T$  to  $1.25\omega_T$  as  $T$  increases from  $0.5T_{co}$  to  $0.85T_{co}$ . The second sound analog of this mode in spherical trap is the ( $\ell = 2, n_2 = 0$ ) mode, which also drops from about  $1.4\omega_T$  to about  $1.35\omega_T$  as  $T$  increases from  $0.5T_{co}$  to  $0.85T_{co}$ .

While we do not expect perfect agreement of our results with the JILA observations [2] because of the difference in trap symmetry and particle numbers, the qualitative and quantitative consistency over the temperature and angular momentum range mentioned above are striking. The above discussions suggest that the ( $m = 0$ ) and ( $m = 2$ ) modes observed below  $T_c$  [2] are the analogs of the second sound modes of layer systems. It is not clear at present why the first sound modes do not appear with great prominence below  $T_c$ . Whether it is due to the way that the modes are excited or due to the fact that density oscillations below  $T_c$  might contain a large second sound component because of the large temperature fluctuations in the second sound modes [as mentioned in discussion (5) above] will be studied later. To clearly identify the nature of the sound modes, it is necessary to experimentally investigate a larger number of modes so as to have more consistency checks with the hydrodynamic predictions. We hope that this work will stimulate and provide guidance for future experiments.

We thank A. Griffin and E. Zaremba for discussions on the dipolar second sound [3], Allan McLeod for providing the programs on  $g_\nu$ , and Vijay Shenoy and Shiwei Zhang for discussions on numerical methods. This work is supported by NSF Grant No. DMR-9705295 and a NASA grant awarded to T. L. H.

- 
- [1] M.H. Anderson *et al.*, Science **269**, 198 (1995); C.C. Bradley *et al.*, Phys. Rev. Lett. **75**, 1687 (1995); K.B. Davis *et al.*, Phys. Rev. Lett. **75**, 3969 (1995).
  - [2] D.S. Jin *et al.*, Phys. Rev. Lett. **78**, 764 (1997).
  - [3] G.M. Kavoulakis, C.J. Pethick, and H. Smith (cond-mat/9710130) have shown that  $10^7$  atoms are needed to reach the hydrodynamic limit near  $T_c$  for the Colorado trap.
  - [4] Recently, E. Zaremba, A. Griffin, and T. Nikuni (cond-mat/9705134) have derived the hydrodynamic equations microscopically in the Popov approximation and have found separate conservation of superfluid and normal densities. They have used a variational method to obtain the ( $\ell = 1, n_2 = 0$ ) second sound for the first time. They find that they normal and supercurrents oscillations cancel each other with frequencies falling below the trap frequency as  $T \rightarrow T_c$ . The characters of the second sound we have found are very different. [See main results section and discussion (3) and (4).]
  - [5] S.J. Putterman, *Superfluid Hydrodynamics* (North-Holland, Amsterdam, 1974), Chap. I, Sec. 4.
  - [6] T.T. Chou, C.N. Yang, and L.H. Yu, Phys. Rev. A **53**, 4257 (1996).
  - [7] T.D. Lee and C.N. Yang, Phys. Rev. **112**, 1419 (1958).
  - [8] Both  $\omega_{\ell \neq 0, n_1 = 0}^{(1)}$  and  $\omega_{\ell \neq 0, n_1 = 1}^{(1)}$  modes were also found by A. Griffin, W. Wu, and S. Stringari, Phys. Rev. Lett. **78**, 1838 (1997) for the *ideal* Bose gas above  $T_c$ . Interaction effects and the behavior of these modes below  $T_c$  were, however, not investigated.
  - [9] T.D. Lee and C.N. Yang, Phys. Rev. **6**, 1406 (1959). Also see A. Griffin, and E. Zaremba, cond-mat/9707058.